

# Enhanced Power Conversion Efficiency of the P3BT (Poly-3-Butyl Thiophene) Doped Nanocomposites of Gd-TiO<sub>3</sub> as Working Electrode



Vinayak Adimule, Santosh S. Nandi,  
and Adarsha Haramballi Jagadeesha Gowda

**Abstract** In this research, we described the enhanced PCE (power conversion efficiency) of the hybrid nanocomposites synthesized by co precipitation and ultrasonic assisted synthesis (UAS). The hybrid nanocomposites fabricated by varying the P3BT (poly-3-butyl thiophene) (5–10% wt ratio)/ Gd-TiO<sub>3</sub>. Their characteristics features were understood by SEM–EDS and HR-TEM, compositional analysis by XRD and band gap calculations by UV–visible and cyclic voltammetry. The hybrid NCs were fabricated either by RF Sputtering with the top contact of Cu/Ag thin deposition, and in the present investigation it is made in the form of a pellet with varying concentrations of P3BT/Gd-TiO<sub>3</sub> which were (pelletized) made as layer of conducting surface with different thickness (100 nm, 250 nm and 550 nm). Photovoltaic (PV) current–voltage characteristics measured by Hg excitation method using Hg probe controller. The fabricated hybrid nanocomposites were studied their effect on the power conversion efficiency of the P3BT doped Gd-TiO<sub>3</sub> in dark and in light illumination. The photovoltaic and current–voltage characteristics is done using Hg-MDC probe controller with The PCE of the (10% wt ratio) of the P3BT doped with Gd-TiO<sub>3</sub> hybrid nanocomposites were 4.18% higher than inorganic Gd-TiO<sub>3</sub> nanocomposites as compared with the other working electrodes. The hybrid NCs showed excellent PV characteristics as compared with the existing inorganic/organic hybrid nanocomposites.

**Keywords** Hybrid Nanocomposites · Power conversion efficiency · Photovoltaic · Current–voltage characteristics · Co-precipitation

---

V. Adimule (✉)

Angadi Institute of Technology and Management (AITM), Savagaon Road, Belagavi 5800321, Karnataka, India

S. S. Nandi

Chemistry Section, Department of Engineering Science and Humanities, KLE Dr. M. S. Sheshgiri College of Engineering and Technology, Udyambhag, Belagavi 590008, Karnataka, India

A. H. Jagadeesha Gowda

Research Scholar, Centre for Research in Medical Devices, National University of Ireland, Gaillimh Galway-H91TK33, Ireland

e-mail: [a.hj1@nuigalway.ie](mailto:a.hj1@nuigalway.ie)

## 1 Introduction

Nano particles isolated through surfactant and capping agents [1, 2], subsequent precipitation is a simple and cost effective method for the isolation of the uniform sized nanocomposites. The polymeric matrices preparation of nanocomposites are based on the structure of the polymer, solvent used such as tetra hydro furan, 1, 4-dioxan, methyl nitrile and acetone which are used in laboratory scale in the preparation of polymer nanocomposites [3–5]. Particle size of the majority nanoparticles mostly in the nanometers size ranging from 10 to 100 nm. The main advantage in the co precipitation method [6–8] is to maintain uniform particle size, solvent stability, stability of the isolated nanocomposites etc. The most of the organic/inorganic hybrid nanocomposites undergo self-assembling in its structure during precipitation, which results in particle agglomeration in the solution. Such hybrid nanocomposites [9, 10] were used most often for solar cells [11], Bio imaging [12], photodiodes [13], sensors [14], dye encapsulates [15], drug delivery materials [16–18]. The imaging process nanoparticles dispersed in solution must have stability towards particle agglomeration, polymeric conjugated hybrid inorganic/organic nanoparticles have been used for photodiodes, batteries, solar cell applications [19, 20], but in contrast to their synthesis, towards isolation, purification and its stability several approaches were adapted for the dispersion of P3BT kind of molecules inside the inorganic particle matrix. The drawbacks of such P3BT: GT nanocomposite synthesis includes expensive processes, scaling up issues and difficult multistep synthesis [21–24]. The present research focuses the study to establish a simple protocol for the synthesis of P3BT: GT hybrid conjugated nanocomposites with highly conjugating donor molecule as P3BT (poly-3-butyl thiophene) and highly accepting inorganic matrix as GT (Gadolinium Titanate) by coprecipitation method under highly acidic condition at higher temperature [25–27]. The calcinated powders of different molar ratios of the P3BT doped hybrid nanomaterials were characterized by CV, SEM, XRD and studied I–V characteristics using Hg excitation method [28–30]. The hybrid nanocomposites also possess stability towards aqueous solution and mixed polar and non-polar solvents. A few current–voltage and capacitance voltage measurements carried out for the fabricated materials of 10% doped P3BT with different thickness of the pellet ranging from 100 to 550 nm in size. A nonlinear relation between the current and the voltage has been reported for the P3BT: GT nanocomposites as well as capacitance–voltage [31]. The assimilated values obtained from the graph was nonlinear and calculated admittance, power dissipation factor and PCE of the P3BT (10%) doped to GT nanocomposites and tabulated. High quantum yield, high solvent susceptibility, photo stability of the hybrid material is due to the dislocation of  $\Pi$  electrons into the inorganic tetrahedral structure and increased addition of P3BT resulted the increased electron carrier and dislocation capacity of the organic polymer in the form of  $\Pi$ - $\Pi$  interactions [32, 33]. The hydrophobic interactions resulted the increased photoemission from the conducting surface of the 10% doped P3BT hybrid solar cells which combine both organic and inorganic semiconductors in an active layer due to increased electron excitation and dissociation at the interface, high stability,

inhibition towards the recombination of generated photo holes and the electrons. The distinct strategies involved in this research work open up varieties of electrical and electronic properties of the hybrid nanomaterials with unique properties. The material finds diversified applications in the solar cells, photodiodes, photo resistance, LEDs, micro sensors, diodes and super capacitor.

## 2 Materials and Methods

Starting chemicals, reagents purchased from e-Merck, India Ltd, Sigma-Aldrich India and from spectro chem. Ltd. JEOL instrument JSM IT-800 supported with hybrid lens and fitted versatile backscattered electron detector (VBED) was used to record the SEM morphology of the samples. XRD Instrument from Bruker D2 Phaser having reciprocal phase mapping and small angle X-ray scattering (SAXS), Cu-K $\alpha$  radiation ( $\lambda = 0.1542$  nm) operating at 50 kV. CHI (Austin) instrument model D630 electrochemical analyzer used for recording CV spectrum and Specord 210 plus with variable resolution and double beam detection was used for optical absorptivity investigation. Pure and Gd doped NS coated as thin films and obtained these films by using electron beam evaporation and the distance between source and the target was 8 cm. the deposited thickness was measured. Mercury Probe Controller MDCs model 802 B was used for I–V of solar cell properties. The 99.98% pure P3BT has been procured from the Sigma Aldrich for doping into the inorganic NCs.

### 2.1 Hg Probe Station (*Hg-Photovoltaic Current–Voltage Method*)

Hg-probe is commonly used for I–V characterization because of its rapid and nondestructive nature. In order to measure the semiconductor properties especially current and voltage, the Hg probe finds its application otherwise classical fabrication was time consuming, needs metallic contact to be established and has several processing steps for the sample to be investigated. The entire processing takes usually several hours and affects the device performance under sun illumination. Hg-probe connects to the well-defined area of the flat sample and if the sample contact is rectifying it can be used to measure resistance, leakage currents etc. The thin films can be of any material either it may be metal, semiconductor or may be oxide. Typical Hg-probe can be used to measure I–V instead of fabricating material over ITO/FTO which intern reduces time and effort. Depending on the contact established between Hg and sample and obtained ohmic and added a value of Hg probe contact is that it is non-destructive and can be easily lifted from the sample.

## 2.2 Determination of I–V/C–V Using Hg-Probe (General Methodologies)

Two different ways of operating Hg-probe commonly categorized Front-Back Contact and Dual Front Contact. Back surface is coated with low resistance metal or alloy and top contact made with suction pump. Total connected area of Hg which is connected to LCR meter for I–V, C–V investigation. Commonly ohmic (rectifying) and non ohmic (Schoty) behavior studied using Hg probe.

Calibration of Hg-Probe.

Hg-probe usually calibrated by capacitance measurement on dielectric film of unknown thickness and permittivity. Hg forms MOS (metal oxide semiconductor structure) which is connected by shielded cables on the LCR meter which intern superimposes a small AC signal of 15 mV.

$$C = \epsilon_0 k A / d$$

K is relative permittivity of the dielectric sample,  $\epsilon_0$  permittivity of free space, A is the area of the dielectric sample and d is the thickness of the dielectric sample. The contact area of Hg can be calculated by.

$$A = C d / k \epsilon_0 .$$

## 3 Experimentation

### 3.1 Synthesis of Gd-TiO<sub>3</sub> NCs (Step 1)

Gd (NO<sub>3</sub>)<sub>3</sub> · 6H<sub>2</sub>O (10–40% molar wt. ratio) and TiCl<sub>4</sub> (titanium tetrachloride) were dissolved in 25 ml of deionized water (DM), treated with 10 ml of concentrated HCl under stirring, CTAB (0.210 g) and triethanol amine (0.5 mL) are added and reaction mixture (RM) was heated to 85°C for 2–3 h. RM was cooled, precipitate obtained after slow addition of NH<sub>4</sub>OH solution was subjected to ultra-sonication for 2 h, precipitate was filtered, washed with cold water and dried at 100–200°C, calcinated at 800–850°C, grounded as powdered Gd-TiO<sub>3</sub> NS.

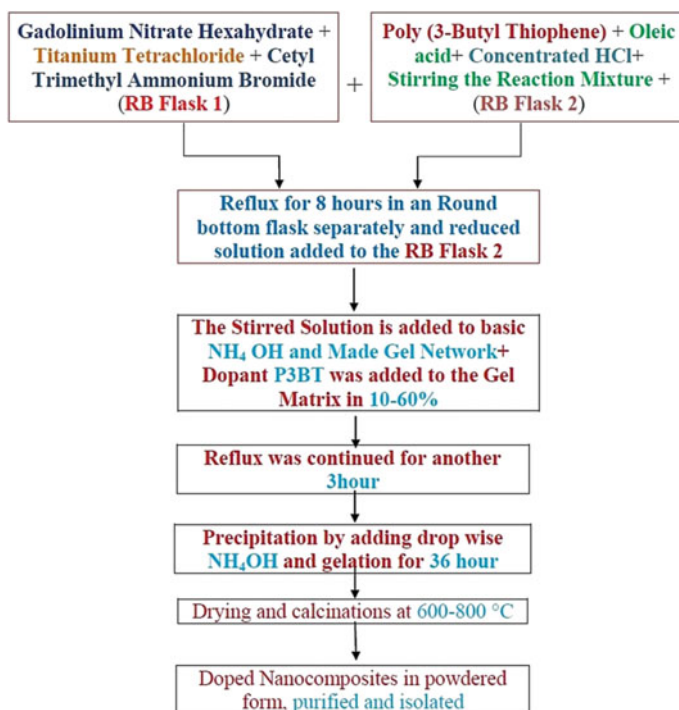


**Fig. 1** Schematic reaction flow chart for the synthesis of P3BT: GTs of NCs

### 3.2 Doping of P3BT (Poly-3-Butyl Thiophene) to Gadolinium Titanate Nanomatrix (Step 2)

Gd TiO<sub>3</sub> (1.43 g, 1 molar ratio, step 1) mixed with P3BT (1.66 g, 10% molar ratio wt. ratio) in 50 ml deionized water and stirred continuously for 1 h. NaOH (4 M) solution was added drop wise up to pH = 9 and heated to 70 °C for 3–4 h. Finally the pale brown precipitate was filtered, washed with cold water, ethanol, dried at 100–200 °C, calcinated at 750–800 °C yielded as fine powders. Figure 1 indicates schematic Reaction Flow chart for the synthesis of P3BT: GTs of NCs.

## 4 Results and Discussion

### 4.1 BHJ Hybrid Working Principles

Solar cells composed off hybrid organic/inorganic nanomaterials reported in the literature generally consists of device architecture fabricated with active layers, top

contact and a bottom contact with the conducting polymer sandwiched in between active components (Fig. 2). Indium tin oxide (ITO) coated as conducting electrode behaving as anode with high work function over flexible plastic or a glass plate with  $100 \Omega/\text{sq cm}^2$  resistance. The polymer poly (3, 4-alkenedioxythiophenes): poly (styrenesulfonate) (PEDOT: PSS) used as hole extractor in between the HTL and ETL layers coated either by spin coating over ITO substrate to form a thin film 100–200 nm thick. Al, Ag metal deposited over photo active layer as cathode and electrons, holes transported via percolating pathways. The holes are transported through the conjugated polymer, and the electrons are transported through the inorganic semiconductor (Fig. 3).

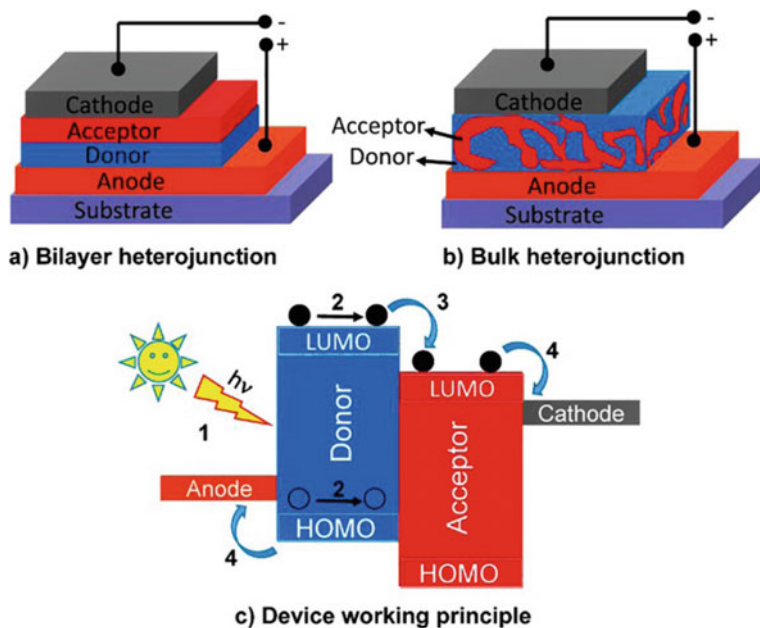
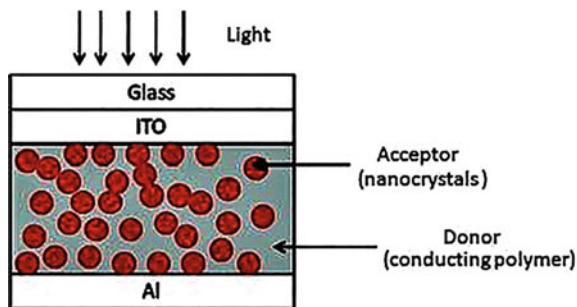
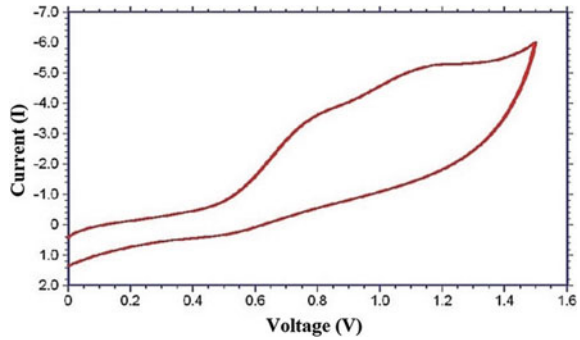


Fig. 2 Schematic conventional fabrication of the solar cell devices as reported in the literature

Fig. 3 Schematic illustration of the interface of the hole and electron charge carries at the boundary



**Fig. 4** Typical illustration of the 10% P3BT doped GT NCs CV spectrum



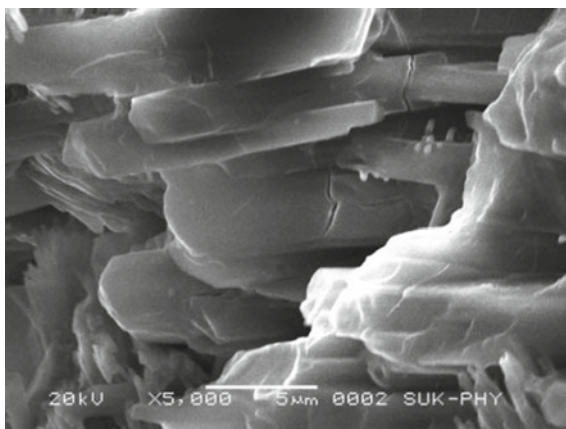
#### 4.2 Electrochemical CV Measurements BHJ Hybrid Working Principles

Redox potentials were recorded using cyclic voltamogram (Fig. 4) the oxidation potential for the highest doped 10% of P3BT was found to be  $-0.44$  eV and reduction potential of  $+0.012$  eV. Applied voltage varied in between 0.5 and 1.4 V. HTL (hole transport layer) acting cathode material is GT and the acting anode material is P3BT (donor), due to the increased donating ability of the P3BT doped to the inorganic NCs which creates band gap of 0.97 eV. Due to electron releasing ability of P3BT organic compound which leads to more negative potential of the combined inorganic/organic NCs.

#### 4.3 SEM Morphological Features

Scanning electron microscopic images (Fig. 5) of the 10% heavily doped GT NCs arrays and the picture depicts the pore diameter, wall thickness, inter pore distance, and the length of the P3BT: GT NCs are 100 nm, 75 nm, 40 nm and 55 nm respectively. The SEM and the particle configuration were obtained using focused ion beam (FIB). The grain size of the P3BT dispersed particle in the inorganic matrix was found to be 60 nm and the grain boundary distance is 100 nm. As seen from the Fig. 5 the increase in concentration of polymeric matrix, number of aggregates and agglomerates of gadolinium nanoparticles increases with the 10% addition the size of the nanoparticle is in between 30 and 55 nm at 5% it is in between 50 and 120 nm. The P3BT doping on the surface of the bulk hetero junction increases the surface conductivity, optical reflectivity and particles agglomerated inside the cavity of the NCs.

**Fig. 5** Scanning electron microscopic images of the 10% P3BT doped GT NCs



#### 4.4 X-ray Diffraction Spectroscopy

Figure 6 shows the X ray diffraction patterns (XRD) of the P3BT: GT NCs recorded after the thermal annealing at 800°C with diffraction peaks are absorbed at  $2\theta$  values. Prominent peak is utilized to estimate the grain size of the  $\text{GdTiO}_3$  NPs with the help of Scherer equation  $D = K\lambda/\beta\cos\theta$  where  $K$  is constant,  $\lambda = 0.154 \text{ \AA}$  and  $\theta$  is the diffraction angle. The hybrid perovskite layer was amorphous and the crystalline phase was (101), (007), (112), (121), (311), (401) at  $2\theta$  of 23, 24, 26, 27, 29, 31, 33, 36 respectively. The crystallinity and the tetragonal crystal structure of the 10% doped P3BT: GT NCs were confirmed by the dominant peak at (101), (112) corresponding to  $2\theta$  values of 29 and 31 respectively. XRD pattern of tetrahedral geometry of the intense peak  $\text{TiO}_3$  is well matched with the JCPDS file number (39–1359). The formation of hybrid materials is confirmed by X-ray analysis which indicates the superimposition of the peaks of GT and P3BT in NCs.

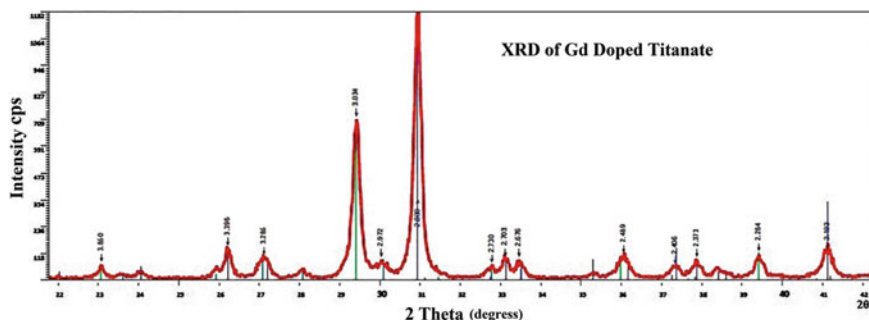
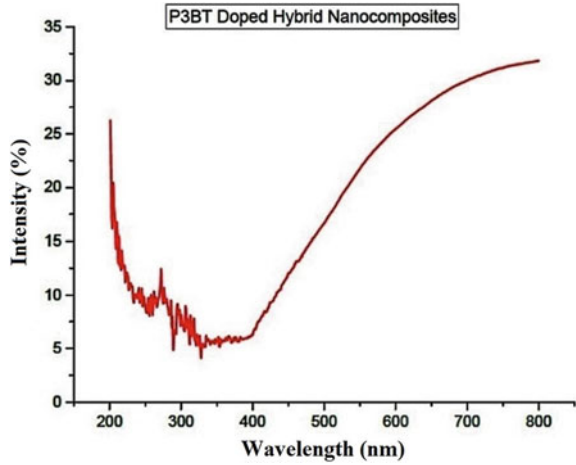


**Fig. 6** XRD pattern of the 10% P3BT doped GT NCs



**Fig. 7** UV–Visible spectrum of the P3BT: GT NCs



### 4.5 UV–Visible Characteristics

Optical absorptivity measured for 10% P3BT doped NCs using UV–Visible spectrophotometer (Fig. 7). NCs dissolved in methanol solvent at room temperature and kept in a special quartz cells irradiated with UV radiation in between 100 and 800 nm. Figure 7 shows the absorption spectra of the 10% P3BT doped GTs with absorptivity in between 450 and 800 nm stretching over end of the visible spectrum. Addition of P3BT (poly-3-butyl thiophene) to Gd-TiO<sub>3</sub> NCs displace the edge of the UV-spectrum and is due to agglomeration of the NPs. UV edge observed at 400 nm, at 305 nm to 400 nm and fall in the in the absorptivity is due to agglomeration of the GTs Chromosphere P3BT addition increases the absorptivity and can be clearly seen from 550 nm. Due to effect of addition of chromospheres P3BT into inorganic gadolinium nanocomposite. Band gap energy of the samples recorded and calculated by Kubeka Mulk model and the direct allowed transition calculated using the formula.

$$(\alpha' h \gamma)^2 = C (h \gamma - E_g).$$

C-is the absorption coefficient,  $h\gamma$ -photon energy and  $E_g$ -optical band gap.

### 4.6 Photovoltaic Current–Voltage Characteristics

Pelletized sample of P3BT: GT NCs were studied for their photo current voltage characteristics and capacitance voltage characteristics using Hg probe, values are tabulated in Tables 1 and 2. The voltage is varied between –4.5 V and 4.5 V for the characteristics graphs to obtain which synchronized with our studies related solar cell properties of nanocomposites. The current gain varies non linearly form –1.36

**Table 1** Depicting the values of current (I), voltage (V) and resistance (R) of the 10% doped P3BT: GT nanoparticles (Fig. 8)

Samples [P3BT, 10%]	Current gain [I]	Voltage applied [V]	Admittance [ $\Omega$ ]
P3BT: GT (P1)	$-1.36 \times 10^{-11}$	-4.4	$3.08 \times 10^{-12}$
P3BT: GT (P2)	$-8.82 \times 10^{-12}$	-3.9	$2.26 \times 10^{-12}$
P3BT: GT (P3)	$1.99 \times 10^{-12}$	-1.3	$-1.53 \times 10^{-12a}$
P3BT: GT (P4)	$1.41 \times 10^{-11}$	3.0	$4.70 \times 10^{-12b}$
P3BT: GT (P5)	$1.48 \times 10^{-11}$	3.4	$4.35 \times 10^{-12}$
P3BT: GT (P6)	$1.89 \times 10^{-11}$	4.5	$4.20 \times 10^{-12}$

<sup>a</sup>(Lowest recorded admittance of the 10% doped GTs); <sup>b</sup>(highest recorded admittance for 10% doped GTs)

$\times 10^{-11}$  A to  $1.99 \times 10^{-12}$  A. The admittance calculated varies from  $-1.53 \times 10^{-12}$  to  $4.70 \times 10^{-12}$  the highest recorded admittance in the present research work for the 10% doped organic material. The dissipation power as calculated varies from  $-2.59 \times 10^{-12}$  to  $8.51 \times 10^{-11}$ . The lowest base line drawn from the summarized results to calculate the Fill factor, Open circuit voltage ( $V_{oc}$ ) which are found to be 1.79 and 0.77 V respectively for the particular 10% doped P3BT material. The power conversion efficiency was found to be 15.2% which is which is 4–5 times higher than the commonly reported for the inorganic perovskite NCs.

## 5 Conclusion

Authors have synthesized the P3BT: GT NCs by co precipitation methods using surfactants and capping agents at high temperature and in highly acidic condition. The method employed by using magnetic stirrer and ultra-sonication and the reducing agent determines the size of the particles as well as the distribution of the particles in the organic/inorganic NCs by taking different wt. ratios of the organic material P3BT. Particle size, agglomeration, distribution and their density, shape was interpreted by SEM and XRD analysis, band gap, oxidation potential ability, reduction nature, absorptivity, optical properties of the doped material experimentally found by using CV and UV–Visible spectrophotometer experiments. Further Current–Voltage (I–V) performance of the 10% doped P3BT: GT NCs BHJ was investigated and after doping 10% wt. ratio of the P3BT to the GT Inorganic NCs showed more efficiency than the inorganic perovskite nanomaterials. The increased efficiency and the fill factor, power conversion efficiency is due to increased addition of P3BT into NCs This research work opens up to synthesize the novel small and large molecular weight of the thiophene compounds into inorganic NCs for efficient materials for the LEDs,

**Table 2** Depicting the values of dissipations power, open circuit potential, Fill factor and efficiency of the maximum doped 10% doped P3BT: GT nanoparticles

Samples [P3BT, 10%]	Dissipation power	Voc [V]	FF	PCE [%]
P3BT: GT (P1)	$5.97 \times 10^{-11}$	0.55	0.87	3.28
P3BT: GT (P2)	$3.44 \times 10^{-12}$	0.88	1.62	4.12
P3BT: GT (P3)	$-2.59 \times 10^{-12}$	0.61	0.47	6.38
P3BT: GT (P4)	$4.24 \times 10^{-11}$	0.77	1.79	15.2
P3BT: GT (P5)	$5.03 \times 10^{-11}$	0.78	0.95	7.89
P3BT: GT (P6)	$8.51 \times 10^{-11}$	0.75	0.32	5.23

<sup>a</sup>(Lowest recorded admittance of the 10% doped GTs); <sup>b</sup>(highest recorded admittance for 10% doped GTs)

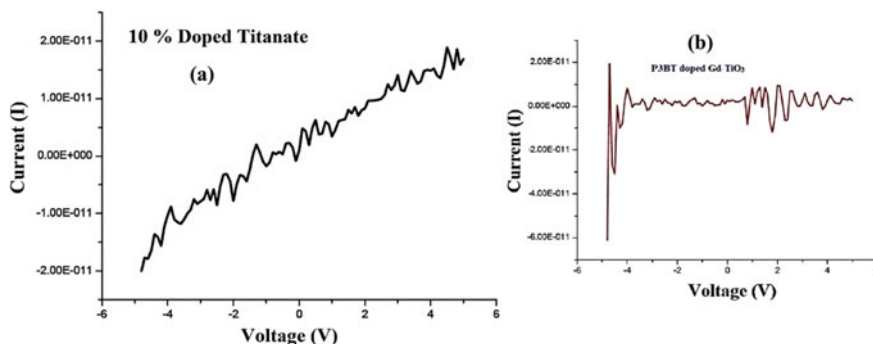


**Fig. 8** a I-V Curve for the 10% doped P3BT: Gd-TiO<sub>3</sub> NCs b photovoltaic I-V Curve for the 10% doped P3BT to Gd-TiO<sub>3</sub> NCs

Photodiodes, sensors and other electrical and electronic components with variable properties.

**Acknowledgements** Author are thankful to KLE IT, Hubballi, CENSE, IISc, Bangalore, MSRIT, Bangalore India necessary experimentation during this research work.

## References

1. Kim JY, Kim SH, Lee HH, Lee K, Ma W, Gong X, Heeger AJ (2006) New architecture for high-efficiency polymer photovoltaic cells using solution-based titanium oxide as an optical spacer. *Adv Mater* 18:572–576
2. Kim JY, Lee K, Coates NE, Moses D, Nguyen TQ, Dante M, Heeger AJ (2007) Efficient tandem polymer solar cells fabricated by all-solution processing. *Science* 317:222–225
3. Sharma GD, Suresh P, Sharma SK, Roy MS (2008) Photovoltaic properties of liquid-state photo electrochemical cells based on PPAT and a composite film of PPAT and Nano crystalline titanium dioxide. *Synth Met* 158:509–515
4. Trznadel M, Zagorska M, Lapkowski M, Louarn G, Lefrant S, Pron A (1996) UV–VIS–NIR and Raman spectro electrochemistry of regioregular poly (3-octylthiophene): comparison with its non-regioregular analogue. *J Chem Soc* 92:1387–1393
5. Shi CJ, Yao Y, Pei QB (2006) Regioregular copolymers of 3-alkoxythiophene and their photovoltaic application. *J Chem Soc* 128:8980–8986
6. Hwang SW, Chen Y (2001) Synthesis and electrochemical and optical properties of novel poly (aryl ether)s with isolated carbazole and p-terphenyl chromophores. *Macromolecules* 34:2981–2986
7. Antonis M, Demetrios B, Giannoulis A, Aquino SD (2016) Design of biodegradable bio-based equilibrium modified atmosphere packaging (EMAP) for fresh fruits and vegetables by using micro-perforated poly-lactic acid (PLA) films. *Postharvest Biol Tec* 111:380–389
8. Rhim JW, Hong SI, Ha CS (2009) Tensile, water vapour barrier and antimicrobial properties of PLA/nanoclay composite films. *Lwt-Food Sci Technol* 42:612–617
9. Reddy JP, Rhim JW (2014) Characterization of bio nanocomposite films prepared with agar and paper-mulberry pulp Nano cellulose. *Carbohydr Polym* 110:480–888

10. Atef M, Rezaei M, Behrooz R (2015) Characterization of physical, mechanical, and antibacterial properties of agar-cellulose bio nanocomposite films incorporated with savory essential oil. *Food Hydrocoll* 45:150–157
11. Choudalakis G, Gotsis AD (2009) Permeability of polymer/clay nanocomposites—a review. *Eur Polym* 45:967–984
12. Heng X, Liang M, Sun S, Shi Y, Ma Z, Sun Z, Xue S (2012) Synthesis and photovoltaic properties of organic sensitizers containing electron-deficient and electron-rich fused thiophene for dye-sensitized solar cells. *Tetrahedron* 68:5375–5385
13. Wang M, Xu M, Shi D, Li R, Gao F, Zhang G, Yi Z, Baker HR, Wang P, Zakeeruddin SM, Gratzel M (2008) High-performance liquid and solid dye-sensitized solar cells based on a novel metal-free organic sensitizer. *Adv Mater* 20:4460–4463
14. Lee MW, Kim JY, Lee DH, Ko MJ (2014) Novel D- $\pi$ -A organic dyes with thieno [3, 2-b] thiophene-3, 4-ethylenedioxythiophene unit as a  $\pi$ -bridge for highly efficient dye-sensitized solar cells with long-term stability. *ACS Appl Mater Interfaces* 6:4102–4108
15. Paek S, Choi H, Choi H, Lee CW, Kang MS, Song K, Nazeeruddin MK, Ko J (2010) Molecular engineering of efficient organic sensitizers incorporating a binary  $\pi$ -conjugated linker unit for dye-sensitized solar cells. *J. Phys. Chem. C* 114:14646–14653
16. Lee MM, Teuscher J, Miyasaka T, Murakami TN, Snaith HJ (2012) Efficient hybrid solar cells based on meso-super structured organo metal halide perovskite. *Science* 338:643–647
17. Etgar L, Gao P, Xue Z, Peng Q, Chandiran AK, Liu B, Nazeeruddin MK, Gratzel M (2012) Mesoscopic  $\text{CH}_3\text{NH}_3\text{PbI}_3/\text{TiO}_2$  heterojunction solar cells. *J Am Chem Soc* 134:17396–17399
18. Burschka J, Pellet N, Moon SJ, Humphry-Baker R, Gao P, Nazeeruddin MK, Gratzel M (2013) Sequential deposition as a route to high-performance perovskite-sensitized solar cells. *Nature* 499:316–319
19. Nie W, Tsai H, Asadpour R, Blancon JC, Neukirch AJ, Gupta G, Crochet JJ, Chhowalla M, Tretiak S, Alam MA (2015) High-efficiency solution-processed perovskite solar cells with millimeter-scale grains. *Science* 347:522–525
20. Mitzi DB, Feild C, Harrison W, Guloy A (1994) Conducting tin halides with a layered organic-based perovskite structure. *Nature* 369:467–469
21. Poglitsch A, Weber D (1987) Dynamic disorder in methylammoniumtrihalogenoplumbates (II) observed by millimeter-wave spectroscopy. *J Chem Phys* 87:6373–6378
22. Im JH, Chung J, Kim SJ, Park NG (2012) Synthesis, structure, and photovoltaic property of a nanocrystalline 2H perovskite-type novel sensitizer  $(\text{CH}_3\text{CH}_2\text{NH}_3) \text{PbI}_3$ . *Nanoscale Res Lett* 7:1–7
23. Baikie T, Fang Y, Kadro JM, Schreyer M, Wei F, Mhaisalkar SG, Graetzel M, White TJ (2013) Synthesis and crystal chemistry of the hybrid perovskite  $(\text{CH}_3\text{NH}_3) \text{PbI}_3$  for solid-state sensitized solar cell applications. *J Mater Chem A*. 1:5628
24. Luk'yanchuk BS, Tribel'ski MI, Ternovski VV (2006) Light scattering at nanoparticles close to plasmon resonance frequencies. *J Opt Technol* 73:371–377
25. Ho WJ, Su SY, Lee YY, Syu HJ, Lin CF (2015) Performance-enhanced textured silicon solar cells based on plasmonic light scattering using silver and indium nanoparticles. *Materials* 8:6668–6676
26. Atwater HA, Albert P (2010) Plasmonics for improved photovoltaic devices. *Nat Mater* 9:205–213
27. Cotal H, Fetzer C, Boisvert J, Kinsey G, King R, Hebert P, Yoon H, Karam N (2009) Multifunction solar cells for concentrating photovoltaic. *Energy Environ Sci* 2:174–192
28. Yamaguchi M, Takamoto T, Araki K, Ekins-Daukes N (2005) Multi-junction III–V solar cells: current status and future potential. *Sol Energy* 79:78–85
29. Yamaguchi M (2002) Multi-junction solar cells and novel structures for solar cell applications. *J High Energy* 14:84–90
30. Pudasaini PR, Ayon AA (2013) Nanostructured plasmonics silicon solar cells. *Microelectron Eng* 110:126–131
31. Shishiyanu ST, Shishiyanu TS, Lupan OI (2006) Temperature effects on gas sensing properties of electrodeposited chlorine doped and undoped n-type cuprous oxide. *Sens Actuators B Chem* 113:468–476

32. White B, Yin M, Hall A (2006) Complete CO oxidation over Cu<sub>2</sub>O nanoparticles supported on silica gel. *Nano Lett* 6:2095–2098
33. Dhas NA, Raj CP (1998) Synthesis, characterization, and properties of metallic copper nanoparticles. *Chem Mater* 10:1446–1452